Acknowledgments. We thank H. P. Mercier and S. Tsai for their help. The Natural Sciences and Engineering Research Council of Canada is thanked for providing operating grants (G.J.S.) and an equipment grant for the X-ray diffractometer (Chemistry Department, University of Toronto), and McMaster University and the Ontario Ministry of Colleges and Universities for the award of a fellowship and scholarships, respectively, to M.B.

(38) *International Tables for X-ray Crystallography*; Ibers, J. A., Hamilton, W. C., Eds.; Kynoch: Birmingham, England, 1974; Vol. 4.

Registry No. 1, 136236-85-6; 2, 136236-87-8; K_2Te, 12142-40-4; Se, 7782-49-2; $TeSSe_2^{2-}$, 136202-30-7; TeS_2Se^{2-}, 136202-29-4; TeS_3^{2-}, 12300-21-9; ^{77}Se, 14681-72-2; ^{125}Te, 14390-73-9; $TeSe_3^{2-}$, 133911-10-1.

Supplementary Material Available: Tables of general temperature factor expressions U_{ij}'s for $TeSe_2^{2-}$ in compound 1 and pyramidal $TeSe_3^{2-}$ in compound 2, bond lengths and bond angles for the 2,2,2-crypt-K^+ cations of compounds 1 and 2, and positional and thermal parameters and selected bond lengths and bond angles for compounds 3 and 4 and stereoviews showing the packing of [2,2,2-crypt-K]$_2$TeSe$_2$·en (1), [2,2,2-crypt-K]$_2$TeSe$_3$·en (2), and [2,2,2-crypt-K]$_2$TeSe$_3$·en (4) (26 pages); tables of final structure factor amplitudes for compounds 1-4 (66 pages). Ordering information is given on any current masthead page.

Contribution from the Dipartimento di Chimica, Università di Firenze, Firenze, Italy

Tetracyanoquinodimethane Salts of Transition-Metal Complexes. 2.[1] Single-Crystal Electron Paramagnetic Resonance of Tris(1,10-phenanthroline)zinc(II) Bis(tetracyanoquinodimethanide) and Tris(1,10-phenanthroline)copper(II) Bis(tetracyanoquinodimethanide)

Alessandro Bencini* and Claudia Zanchini

Received February 7, 1991

The single-crystal and polycrystalline powder EPR spectra of the compounds $Zn(phen)_3(TCNQ)_2$ and $Cu(phen)_3(TCNQ)_2$ have been recorded at the X-band frequency in the temperature range 300-4.2 K. In the Zn derivative, a Frankel-type excitonic spectrum was observed attributed to one of the two magnetically nonequivalent $TCNQ^-$ ions seen in the crystal structure. The triplet exciton spectra were interpreted with a dipolar zero field splitting tensor with $|D_1| = 66\ (2) \times 10^{-4}$ cm^{-1} and $|E_1/D_1| = 0.12\ (1)$. These values nicely agree with the spin density distribution computed with the Xα-SW method. Less intense features seen in the crystal spectra at temperatures lower than 20 K were assigned to a $S = 2$ state arising from exciton-exciton interactions. The zero field splitting of the $S = 2$ state was measured to be $|D_2| = 35\ (2) \times 10^{-4}$ cm^{-1} and $|E_2/D_2| = 0.07\ (1)$. The EPR spectra of $Cu(phen)_3(TCNQ)_2$ showed only resonances due to one unpaired electron localized on a copper(II) center. The spectra have been found to be temperature dependent, the principal g values being $g_x = 2.037\ (3)$, $g_y = 2.052\ (3)$, and $g_z = 2.104\ (3)$ and $g_x = 2.052\ (3)$, $g_y = 2.057\ (3)$, $g_z = 2.180\ (3)$ at 290 and 4.2 K, respectively. This temperature dependence has been attributed to interactions of the copper(II) ion unpaired electron with the mobile triplet excitons of $TCNQ^-$.

Introduction

The number of compounds containing TCNQ (TCNQ = tetracyanoquinodimethane) and related molecules and transition-metal or organometallic complexes is increasing day after day, and most of these solids have shown unusual magnetic and/or charge conduction properties.[2-5] In the majority of these compounds, the nonorganic part plays an important role in determining the arrangement of the TCNQ molecules in the solid and, often, in governing a partial transfer of charge to the TCNQ. Examples of these compounds range from the simple alkali-metal salts of $TCNQ^-$, either containing TCNQ radicals with a 1- charge or more complex systems like $(TCNQ)_3^{2-}$ anions, to solids in which charged clusters of metals crystallize together with TCNQ molecules.[5-10] An incomplete charge transfer to TCNQ often is associated with electrical conduction, while a complete charge transfer is often associated with peculiar magnetic properties such as the formation of mobile triplet excitons.[7-10]

With the aim to investigate the nature of the interactions between the organic radicals and between the organic and the inorganic parts of the solid, we started a research program devoted to the synthesis and structural and magnetic characterization of TCNQ-containing solids having inorganic parts as simple as possible but undergoing some dynamic effect such as Jahn-Teller distortion or valence delocalization. The main purpose for this is to have simpler systems that could be investigated through the largest number of experimental techniques and having some electronic structure, in the inorganic part, that could modulate the interactions between the organic electrons. As a first attempt, we looked for systems undergoing dynamic Jahn-Teller distortions and we synthesized salts of general formula $M(phen)_3(TCNQ)_2$, where M is a bipositive first-row transition-metal ion and phen is the aromatic ligand 1,10-phenanthroline. The stoichiometry of these solids suggests that the charge transfer between the metal and the TCNQ is complete, and therefore TCNQ is present in the -I oxidation state. No significant electric conduction was

(1) Part 1: Bencini, A.; Midollini, S.; Zanchini, C. *Inorg. Chem.* **1989**, *28*, 1963.
(2) Miller, J. S.; Epstein, A. J. In *Electron Transfer in Biology and the Solid State*; Johnson, M. K., King, R. B., Kurtz, D. M., Jr., Kutal, C., Norton, M. L., Scott, R. A., Eds.; Advances in Chemistry 226; American Chemical Society: Washington, DC, 1990; p 419.
(3) Miller, J. S.; Calabrese, J. C.; Harlow, R. L.; Dixon, D. A.; Zhang, J. H.; Reiff, W. M.; Chittipedi, S.; Selover, M. A.; Epstein, A. J. *J. Am. Chem. Soc.* **1990**, *112*, 5496.
(4) Ward, M. A.; Fagan, P. J.; Calabrese, J. C.; Johnson, D. C. *J. Am. Chem. Soc.* **1989**, *111*, 1719.
(5) Endres, H. In *Extended Linear Chain Compounds*; Miller, J. S., Ed.; Plenum Press: New York, 1983, Vol. 3, p 263.
(6) Zeller, H. R. *Adv. Solid State Phys.* **1973**, *13*, 31.
(7) Nordio, P. L., Soos, Z. G.; McConnell, H. M. *Annu. Rev. Phys. Chem.* **1966**, *17*, 237.
(8) Hatfield, W. E. *NATO Conf. Ser. 6* **1979**, *1*, 1.
(9) Soos, Z. G. *Annu. Rev. Phys. Chem.* **1974**, *25*, 121.
(10) Soos, Z. G.; Bondeson, S. R. In *Extended Linear Chain Compounds*; Miller, J. S., Ed.; Plenum Press: New York, 1983, Vol. 3, p 193.

0020-1669/91/1330-4245$02.50/0

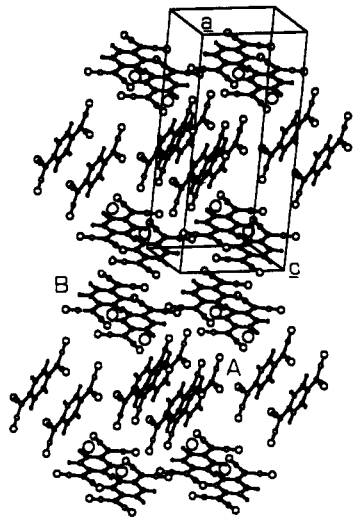

Figure 1. View of the crystal packing of $Zn(phen)_3(TCNQ)_2$. Only the $TCNQ^-$ ions (both A and B types) and the zinc atoms are showed for sake of simplicity.

observed in these compounds. The crystal and molecular structure of the zinc(II) and copper(II) salts have been previously reported.[1] In the crystal structure of both compounds, two nonequivalent dimers of $TCNQ^-$ radical were seen. In one of them, called A,

A

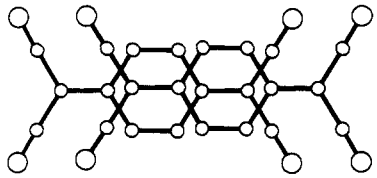

(R–B)

the $TCNQ^-$ ions of each dinuclear unit stack themselves one over the other in the ring-to-external bond (R–B) geometry already observed in a number of simple salts including the alkali-metal salts. In the other dimer, called B, a dinuclear unit was observed with an unusual external bond-to-external bond (B–B) geometry.

B

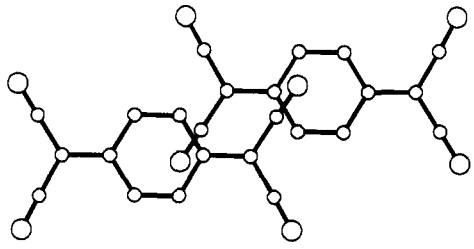

(B – B)

The spatial distribution of these two dimers is such that they are arranged in chains. A view of the crystal packing of the $TCNQ^-$ ions in $Zn(phen)_3(TCNQ)_2$ is given in Figure 1, where the A and B molecules are also labeled. In Figure 1, only the zinc atoms are placed for clarity purposes. The arrangement of the $TCNQ^-$ ions in the copper salt is strictly similar.[1]

The temperature dependence of the magnetic susceptibility of the zinc salt between 300 and 5 K was interpreted[1] with a Heisenberg antiferromagnetic linear-chain model, but only one of the two chains was found to contribute to the magnetic behavior. The magnetic properties of the copper salt were similarly rationalized with the inclusion of a Curie contribution to account

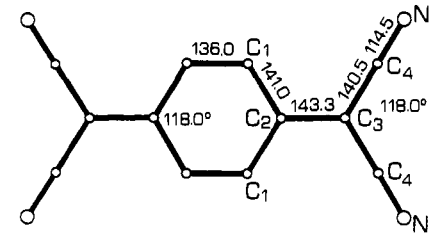

Figure 2. Scheme of the $TCNQ^-$ molecule, having an overall D_{2h} symmetry, with the bond distances (pm) and angles (deg) used in the Xα–SW calculations.

for the paramagnetism of the $Cu(phen)_3^{2+}$ cation. The isotropic exchange parameter, J, was computed to be 60 (2) and 29 (1) cm^{-1} for the zinc and copper salts, respectively, the alternation parameter, α, being 0.8 (1) and 0.6 (1), respectively. $\alpha = 0$ corresponded to an isolated dimeric unit, and $\alpha = 1$, to a regular linear chain.[1] Since the crystal packings of TCNQ and the molecular geometries seen in these two salts are very similar to each other, no immediate explanation of the difference between the two fits is possible, except the fact that the temperature dependence of the magnetic susceptibility of $Cu(phen)_3(TCNQ)_2$ is obscured by the heavier magnetism of the copper(II) complex; in particular, no maximum in the susceptibility curve could be observed and the uncertainty in the J and α values is surely larger than the standard deviation computed through the least-squares procedure.

In order to have a better understanding of the magnetic interactions in these systems, we performed single-crystal EPR measurements on $Zn(phen)_3(TCNQ)_2$ and $Cu(phen)_3(TCNQ)_2$ at variable temperature in the range 300–4.2 K, and we computed the spin densities on the atoms of $TCNQ^-$ with spin-polarized Xα–SW calculations.[11] Surprisingly enough, the EPR spectra of the zinc salts showed, together with resonances due to Frankel triplet excitons, resonances attributable to spin states with $S > 1$, which can arise from the interactions between triplet excitons localized in contiguous sites in the crystal. To the best of our knowledge, this is the first time that exciton–exciton interactions have been directly observed in TCNQ-containing solids.

In the following, we wish to describe in more detail the spectromagnetic properties of the $TCNQ^-$ salts of $Zn(phen)_3^{2+}$ and $Cu(phen)_3^{2+}$.

Experimental Section

Synthesis of the Compounds. The compounds $Zn(phen)_3(TCNQ)_2$ and $Cu(phen)_3(TCNQ)_2$ have been prepared as previously described.[1] Well-formed crystals suitable for single-crystal EPR spectroscopy were obtained directly from the synthetic procedure. The crystals are triclinic, space group $P\bar{1}$, and were found to conform to the structure report[1] with a Philips PW1100 automated diffractometer. The cell parameters are $a = 2197.2$ (5) pm, $b = 1116.4$ (3) pm, $c = 1016.5$ (3) pm, $\alpha = 86.03$ (4)°, $\beta = 84.81$ (6)°, and $\gamma = 83.36$ (3)° for $Zn(phen)_3(TCNQ)_2$ and $a = 2194.5$ (5) pm, $b = 1110.6$ (3) pm, $c = 1018.6$ (3) pm, $\alpha = 86.50$ (4)°, $\beta = 84.41$ (6)°, and $\gamma = 83.21$ (4)° for $Cu(phen)_3(TCNQ)_2$.

EPR Spectra. The EPR spectra have been measured by using a Varian E-9 X-band spectrometer equipped with an Oxford ESR 9 continuous-flow cryostat. The orientation of the crystals in the static magnetic field was changed by placing the crystals on a perspex rod. The magnetic field was calibrated by using DPPH (diphenylpicrylhydrazyl) as a standard.

Computational Details. Molecular orbital calculations on the $TCNQ^-$ ion have been performed by using the Xα scattered wave (SW) approximation[11] with the computer programs previously described.[12] All the calculations were spin unrestricted and the SCF procedure was stopped when the relative change in the potential was 10^{-4} and/or the variation of the energy levels was not more than 0.0001 Ry. The virial ratio, $-2\langle T\rangle/\langle V\rangle$, was 0.9946. An overall D_{2h} symmetry was imposed on the molecule by using the bond distances and angles shown in Figure 2, which represent the average values seen in the $TCNQ^-$ B molecule. The sphere radii were chosen by following the Norman[13] procedure using

(11) Johnson, K. H. *Adv. Quantum Chem.* **1973**, *7*, 143.
(12) Albonico, C.; Bencini, A. *Inorg. Chem.* **1988**, *27*, 1934.
(13) Norman, J. G., Jr. *Mol. Phys.* **1976**, *31*, 1191.

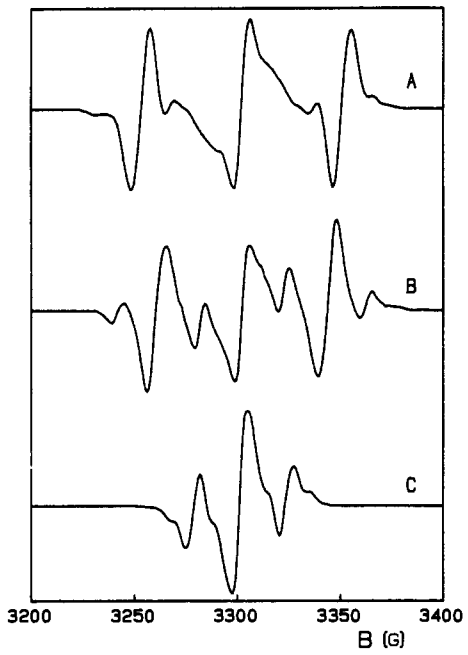

Figure 3. Some representative crystal spectra of $Zn(phen)_3(TCNQ)_2$ recorded at 4.2 K with the static magnetic field: (A) along the X_1 axis; (B) in the Z_1X_1 plane at 50° from X_1; (C) in the X_1Y_1 plane at 30° from X_1.

a reduction factor $R = 0.90$. They are $r(C1) = 91.4$ pm, $r(C2) = 90.5$ pm, $r(C3) = 90.4$ pm, $r(C4) = 87.2$ pm, $r(N) = 93.1$ pm, and $r(H) = 54.0$ pm. A tangent Watson sphere[14] with a +1 charge was used to account for the negative charge of the molecule. The values computed by Schwartz[15] for the free atoms were used in the atomic regions. For the inter- and outer-sphere regions an average of the atomic values according to the valence electron number was used.

Results

EPR Spectra of $Zn(phen)_3(TCNQ)_2$. Single-crystal EPR spectra have been recorded by rotating one crystal around three orthogonal axes X_1, Y_1, and Z_1. The X_1 axis is perpendicular to the (−1, 0, −1) face and Y_1 is parallel to $-b$. At room temperature, an isotropic exchange-narrowed signal is observed in all crystal orientations. When the temperature is decreased, the signal broadens and, at temperatures lower than ≈ 20 K, splits into an isotropic band at $g \approx 2.00$ flanked by two features. When the crystal is cooled at lower temperatures, the splitting between the lateral bands increases, and at temperatures lower than ≈ 6 K additional less intense features appear.

Some representative crystal spectra recorded at 4.2 K are shown in Figure 3. All the observed features, except the central line at $g \approx 2.00$, were found to be dependent on the orientation of the crystal in the static magnetic field.

The polycrystalline powder spectra recorded at 4.2 K showed transitions typical of a $S = 1$ state split by a small zero field splitting,[16] which overlap with a central isotropic line. A sharp half-field transition can be clearly observed. Some less intense features, which cannot be assigned to a single triplet species, were also seen around the central signals.

Since the crystals are triclinic, only one magnetically nonequivalent site is present in the unit cell, and we assigned the two most intense bands seen in the crystal spectra to the two allowed $\Delta M_S = \pm 1$ transition within a $S = 1$ manifold. The angular dependence of the transition fields is reported in Figure 4. This angular dependence was reproduced with the spin Hamiltonian

$$H_S = \mu_B B \cdot \mathbf{g}_S \cdot S + S \cdot \mathbf{D}_S \cdot S \qquad (1)$$

and $S = 1$. The experimental data have been fitted with (1) by using a nonlinear least-squares procedure previously described[17] keeping the $\mathbf{g}_1$ tensor fixed to the isotropic value 2.002. The best fitting parameters are reported in Table I, and the results of the fitting are shown as solid lines in Figure 4. The z direction of the zero field splitting tensor, $\mathbf{D}_1$, i.e. the direction of maximum zero field splitting, makes an angle of ≈ 13° with the line joining the centers of the aromatic rings of the B-type dimer (see Figure 5) and ≈45° with the line joining the centers of the aromatic rings of the A-type dimers.

Table I. Principal Values[a] and Directions[b] of the $\mathbf{D}_1$ and $\mathbf{D}_2$ Tensors for $Zn(phen)_3(TCNQ)_2$ and of the Room-Temperature and 4.2 K $\mathbf{g}$ Tensors for $Cu(phen)_3(TCNQ)_2$

$Zn(phen)_3(TCNQ)_2$		
D_{1x}	D_{1y}	D_{1z}
0.0014 (1)	0.0030 (1)	−0.0044 (1)
0.03 (1)	0.459 (7)	0.887 (3)
−0.96 (1)	0.25 (4)	−0.09 (1)
−0.27 (3)	−0.85 (1)	0.451 (6)
D_{2x}	D_{2y}	D_{2z}
0.0009 (1)	0.0014 (1)	−0.0023 (1)
0.03 (1)	0.478 (8)	0.878 (2)
−0.99 (2)	0.12 (3)	−0.06 (1)
−0.14 (3)	−0.87 (1)	0.474 (5)
$Cu(phen)_3(TCNQ)_2$		
g_x	g_y	g_z
Room Temperature		
2.037 (3)	2.052 (3)	2.104 (3)
0.53 (4)	0.43 (5)	−0.73 (1)
−0.37 (7)	−0.66 (4)	−0.66 (2)
0.76 (6)	−0.62 (8)	0.19 (3)
4.2 K		
2.052 (3)	2.057 (3)	2.180 (3)
−0.5 (2)	0.5 (2)	−0.68 (1)
0.68 (9)	−0.2 (2)	−0.69 (2)
0.5 (3)	0.8 (2)	0.23 (2)

[a] In cm^{-1}. [b] The directions are given as cosines referred to the $X_1Y_1Z_1$ and $X_2Y_2Z_2$ reference frames for $Zn(phen)_3(TCNQ)_2$ and $Cu(phen)_3(TCNQ)_2$, respectively (see text).

The analysis of the temperature dependence of the intensity and position of the triplet lines was found useful in obtaining information on the triplet exciton motion.[18] In the present case, however, the excitonic triplet can be detected only at temperatures lower than 20 K, which cannot be measured with uncertainties lower than 3–4 K on our continuous-flow cryostat, so that we were not able to obtain variable temperature data with sufficient accuracy.

The less intense bands observed in the crystal spectra overlap with the triplet signals in most crystal orientations, and we could not follow their angular dependence in all the three orthogonal rotations. In most cases, it has been possible to estimate only the positions of the lowest and highest field bands. The angular dependence of the observed bands is shown in Figure 6. It has to be noted that in the Y_1 rotation, where the four bands show the maximum splitting, a series of four equally spaced bands is observed in some crystal orientations. It is not possible to safely affirm if this structure is maintained in all of the other spectra. In order to assign these transitions, we have taken into account the possibility of a structural phase transition, which could yield to two types of dimers with slightly different J and D values, and we tried to fit the extra lines like two independent triplet species, but no reasonable fit was obtained. As a last possibility, we assigned the observed bands to transitions between a $S = 2$ state split by a zero field splitting much smaller than the Zeeman term. We fitted them by using a linear least-squares procedure based on a first-order expression of the transition fields[16] obtained by H_S, putting $S = 2$. The results of the fitting are graphically

(14) Watson, R. E. *Phys. Rev.* **1958**, *111*, 1108.
(15) Schwartz, K. *Phys. Rev. B* **1972**, *5*, 2466.
(16) Bencini, A.; Gatteschi, D. In *Transition Metal Chemistry*; Melson, G. A., Figgis, B. N., Eds.; Marcel Dekker: New York, 1982, Vol. 8, p 1.
(17) Banci, L.; Bencini, A.; Gatteschi, D.; Zanchini, C. *J. Magn. Reson.* **1982**, *48*, 9.
(18) Bencini, A.; Gatteschi, D. *Electron Paramagnetic Resonance of Exchange Coupled Systems*; Springer Verlag: Heidelberg, 1990.

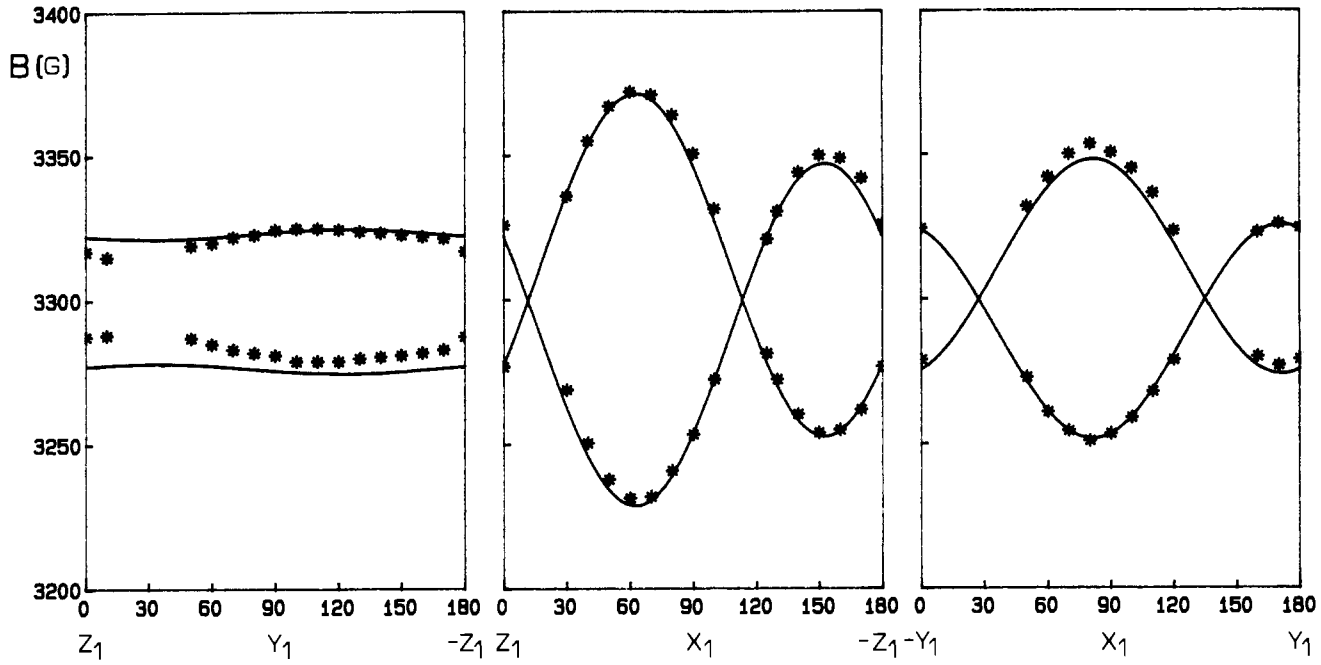

Figure 4. Angular dependence of the observed transition fields for $Zn(phen)_3(TCNQ)_2$. The solid line represents the best fitting curves (see text).

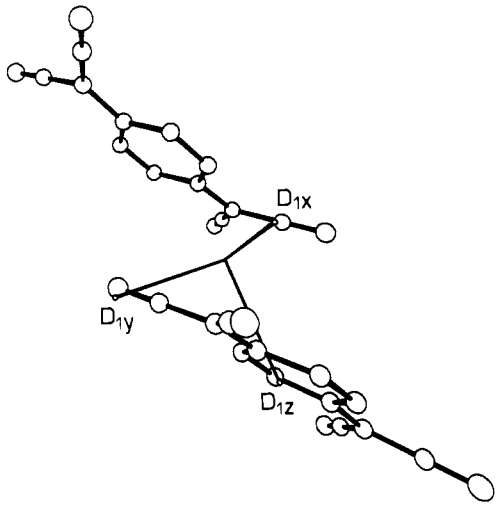

Figure 5. Orientation of the $\mathbf{D}_1$ tensor for $Zn(phen)_3(TCNQ)_2$ in the molecular frame of the B-type $TCNQ^-$ dimer.

represented in Figure 6 as solid lines. In Figure 6 the computed other two possible transitions arising from the $S = 2$ state are shown, and the observed positions of the inner bands, not included in the fitting procedure, are represented as open circles. The $\mathbf{D}_2$ tensor obtained as the best fit is reported in Table I. Since the $\mathbf{g}_2$ tensor is isotropic at $g = 2.00$, within experimental error, the computed principal directions of $\mathbf{g}_2$ are affected by a large error and are not shown in Table I. The principal directions of $\mathbf{D}_2$ are parallel, well within experimental errors, to those of the zero field splitting tensor of the triplet state, $\mathbf{D}_1$.

EPR Spectra of $Cu(phen)_3(TCNQ)_2$. Representative polycrystalline powder spectra of $Cu(phen)_3(TCNQ)_2$ recorded at temperatures between 300 and 4.2 K are shown in Figure 7. Two features are apparent: first, no signal at $g \approx 2.00$ attributable to $TCNQ^-$ radicals is observed; second, the spectra show a temperature dependence. The 300 K spectrum can be interpreted by using an $S = {}^1/_2$ spin Hamiltonian with $g_1 = 2.12$, $g_2 = 2.06$, and $g_3 = 2.04$. A continuous change in the principal g values is observed on decreasing the temperature, and at 4.2 K the g values are $g_\parallel = 2.26$ and $g_\perp = 2.05$.

Single-crystal spectra were recorded, at both 300 and 4.2 K, by rotating one crystal around three orthogonal laboratory axes X_2, Y_2, and Z_2 with Z_2 parallel to the $-b$ axis and X_2 perpendicular to the $(-1, 0, -1)$ face. In any case, only one resonance, attributed to a $S = {}^1/_2$ effective spin, was observed, whose angular dependence is shown in Figure 8. The data have been fitted through a least-squares procedure using the Schönland method.[19] The results of the fitting are given in Table I.

Xα–SW Calculations. The spin densities computed for the $TCNQ^-$ anion are reported in Table II and compared with the results of other calculations. Since the present values are quite different from those previously used by several authors to compute the zero field splitting parameters observed in $Rb(TCNQ)_2$,[18] although the geometrical and bonding parameters of $TCNQ^-$ are equal within experimental error in the rubidium and in the zinc salts, we used the zero field splitting tensor of the rubidium compound as a check of the quality of the actual values of the spin densities. If the generalization of the point dipolar approximation is used, the zero field splitting tensor is computed as

$$D_{ij} = {}^1/_2 g^2 \mu^2_B \sum_{\alpha\beta} \rho_\alpha \rho_\beta (r_{\alpha\beta}^2 \delta_{\alpha\beta} - 3 i_{\alpha\beta} j_{\alpha\beta}) r_{\alpha\beta}^{-5} \qquad (2)$$

where $i, j = x, y, z$ and ρ_α and ρ_β are the spin densities for atoms α on molecule 1 and for atom β on molecule 2. $r_{\alpha\beta}$ is the distance between atoms α and β. The computed values for $Rb(TCNQ)_2$ are $D = {}^3/_2 D_{zz} = -0.0102$ cm^{-1} and $E/D = 0.11$ to be compared with the experimental ones $|D| = 0.0131$ cm^{-1} and $|E/D| = 0.12$. These values were simply compared with literature reports, without trying to optimize the spin density parameters by using a fitting procedure. Contrary to the results previously obtained, we compute a D value which is smaller than that experimentally observed. The E/D ratio is however in excellent agreement with the experiment.

Using the above spin densities, we computed, for the B-type dimer of the $Zn(phen)_3^{2+}$ salt, $D_1 = -0.0048$ cm^{-1} and $E_1/D_1 = 0.10$, which must be compared with the experimental values $|D_1| = 0.0066$ (2) and $|E_1/D_1| = 0.12$ (1). Again a D value smaller than the experimental one is computed. In Table II, we report also the spin densities already used for $TCNQ^-$ and the values of D_2 and E_2/D_2 computed as described in the next section.

Discussion

The temperature dependence of the EPR spectra of $Zn(phen)_3(TCNQ)_2$ is typical of a triplet exciton of the Frankel type,[18,20,21] which localizes at temperatures lower than 20 K.

(19) Schönland, R. S. *Proc. Phys. Soc.* **1959**, *73*, 788.
(20) Chestnut, D. B.; Phillips, W. D. *J. Chem. Phys.* **1961**, *35*, 1002.
(21) Chestnut, D. B.; Arthur, P. *J. Chem. Phys.* **1962**, *36*, 2969.

Table II. Spin Densities ρ_i Computed for an Isolated $TCNQ^-$ Ion Radical and Zero Field Splitting Parameters Calculated for the B-Type Dimer in $Zn(phen)_3(TCNQ)_2$

ρ_1	ρ_2	ρ_3	ρ_4	ρ_N	D_1[a]	E_1/D_1	D_2[a]	E_2/D_2	ref
0.045	0.056	0.225	−0.003	0.067	−0.0075	0.12			27
0.057	0.067	0.219	0.009	0.040	−0.0090	0.10			28
0.059	0.109	0.191	0.002	0.039	−0.0095	0.083			29
0.061	0.132	0.180	0.001	0.031	−0.0099	0.075			30
0.0336	0.0746	0.1565	−0.0068	0.0413	−0.0048	0.100	−0.0018	0.15	*b*

[a] In cm^{-1}. [b] This work.

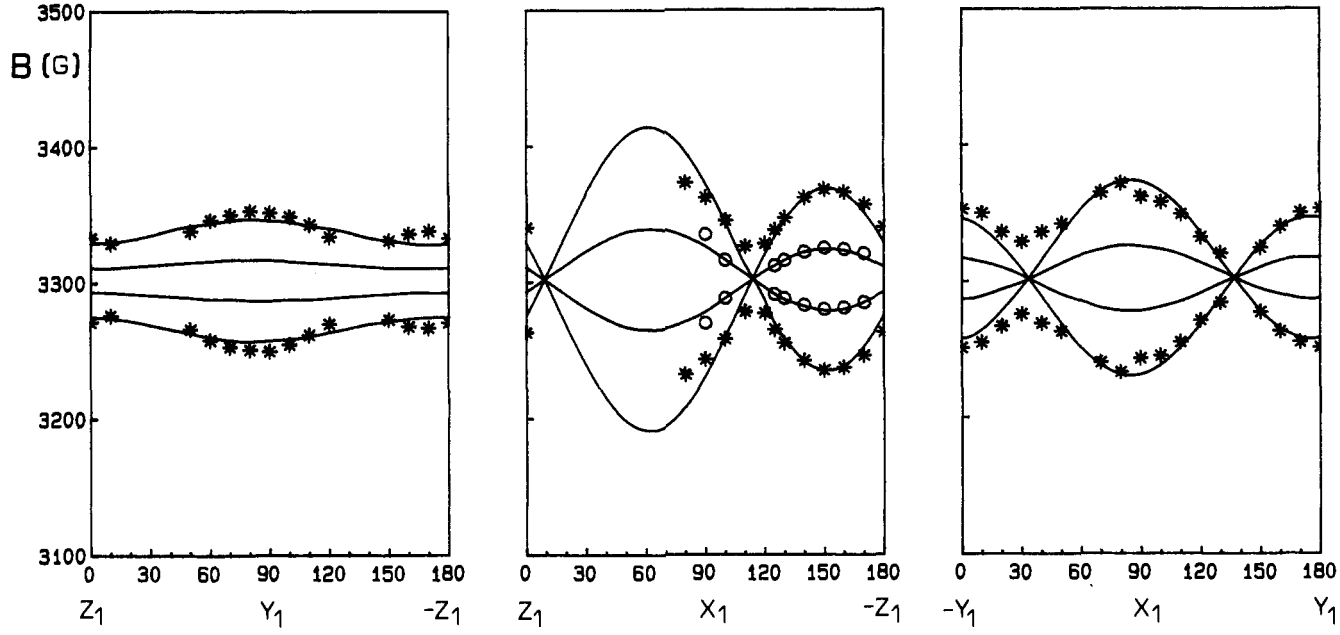

Figure 6. Angular dependence of the transitions fields for a S = 2 state (see text) for $Zn(phen)_3(TCNQ)_2$. The observed outer bands (✱) and inner bands (O) are also indicated.

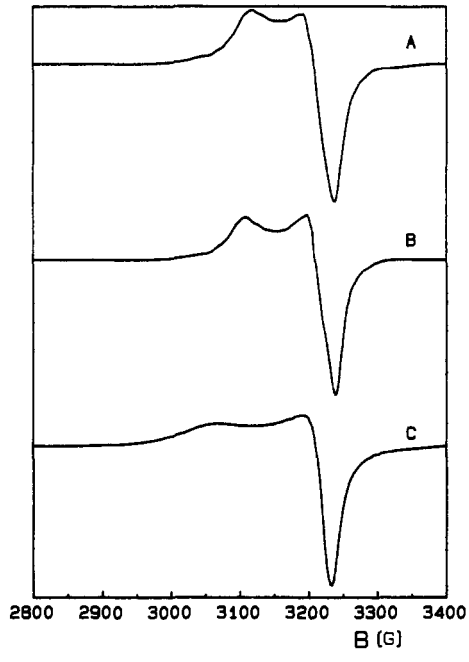

Figure 7. Some polycrystalline powder spectra of $Cu(phen)_3(TCNQ)_2$ recorded at (A) room temperature (300 K), (B) 170 K, and (C) 4.2 K.

Similar excitons, which arise from the interactions between the spins on two adjacent molecules, have been observed in a number of TCNQ-containing solids in which the TCNQ pair was bound in the R–B mode, as well as in σ-type TCNQ dimers.[10,22,23] In all of the previously reported cases, the interactions between the ions and the local lattice distortions, which favor the localization of the exciton along the chain, were strong enough to give localization temperatures around 77 K. In the present case, the exciton mobility is larger and they localize only at temperatures lower than 20 K. The relatively large values of ΔB_{pp}, which range from 10 to 20 G, can be attributed to unresolved hyperfine structure, which is generally considered to result from a dynamic averaging effect from translation or diffusion of excitons through the crystal. Other effects that can contribute to the line width arise from exciton–exciton interactions.

The magnetic susceptibility data have been interpreted with a singlet-triplet separation of ≈ 60 cm^{-1} and clearly indicate that only one of the two crystallographically independent dimers, A and B, is magnetic in the 4.2–300 K temperature range. The single-crystal EPR spectra allowed us to distinguish between the two inequivalent $(TCNQ)_2^{2-}$ dimers. In the present case, the **g** anisotropy is small and the anisotropic exchange contribution to the zero field splitting is expected to be negligible with respect to the main magnetic dipolar interactions, so that the largest component of $\mathbf{D}_1$, D_{1z}, should be directed along the line connecting the two interacting $TCNQ^-$ units of the dimers. As stated in the Results, this is not true for the A-type dimers, but it is true, with a good approximation, for the B-type dimer, which appears to be responsible for the observed spectra. The value of J is much smaller than the values observed in either the σ- or the π-bonded R–B dimer[23] and shows that the present B–B interaction is smaller than the σ and the R–B ones, which usually give rise to singlet-triplet separations of hundreds of wavenumbers.

The observed zero field splitting parameters are smaller than those observed in $Rb_2(TCNQ)_2$ and in σ-bonded dimers. The spin densities computed by using the Xα–SW theory give, using the

(22) Morton, J. R.; Preston, K. F.; Ward, M. D.; Fagan, P. J. *J. Chem. Phys.* **1989**, *90*, 2149.

(23) Hoffmann, S. K.; Corvan, P. J.; Singh, P.; Sethulekshuni, C. N.; Metzger, R. M.; Hatfield, W. E. *J. Am. Chem. Soc.* **1983**, *105*, 4608.

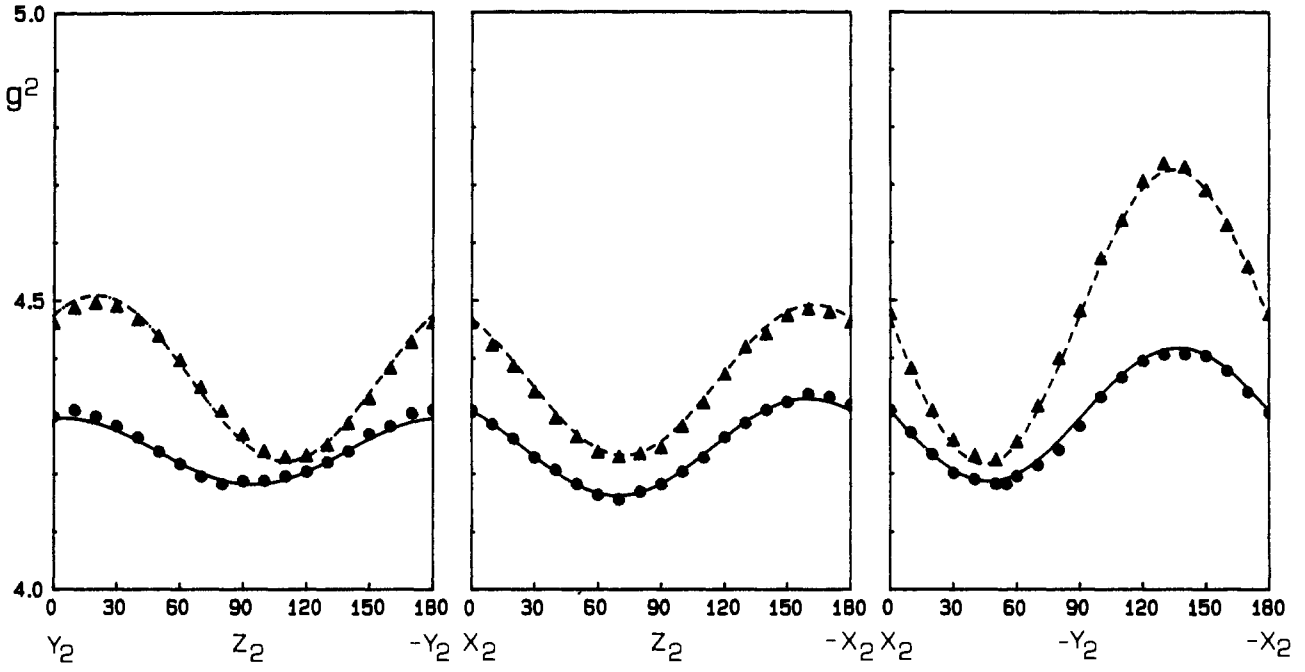

Figure 8. Angular dependence of the g^2 tensor for $Cu(phen)_3(TCNQ)_2$ at 300 K (●) and 4.2 K (▲). Solid and dashed lines represent the best fitting curves obtained with the parameters reported in Table I.

point dipolar approximation, D values that are smaller than those found in $Rb_2(TCNQ)_2$ and in the present case, but the E/D ratio nicely agrees with experiment. As a matter of fact, spin densities computed through other MO methods, which are collected in Table II, always gave D values larger than the experimental values. In any case the differences between the observed and the computed values can be due to the rather crude approximation of the point dipolar model. It should be noted that in the present case we are able to compare the zero field splitting parameters of two $TCNQ^-$ ions in two different geometrical arrangements and the ratio between the D values computed for the Rb^+ and the $Zn(phen)_3^{2+}$ salts (2.12) is only 7% larger than the ratio between the experimental values (1.98). This fact, together with the nice agreement of the computed E/D ratios and the experimental values, probably means that one can be confident in the relative variations in D rather than in the absolute values and that while the point dipolar approximation could be inadequate to quantitative description of the zero field splitting, it can give a reasonable relative estimate of this.

Besides the transitions due to the triplet species, an intense orientation-independent transition at $g \approx 2$ was observed in the crystal spectra. This feature has already been observed in other excitonic systems, and much work has been done to ascertain its nature.[18]

Some novel features appeared in the EPR spectra of the $Zn(phen)_3(TCNQ)_2$ salt as compared to the spectra of other excitonic TCNQ systems, i.e. the transitions, attributed to a $S = 2$ state, which flank the transitions arising from the triplet excitonic state. This state can arise from exchange and/or magnetic dipolar interactions between localized excitons. If this interpretation is correct it is the first time, to the best of our knowledge, that these interactions show measurable effects rather than contribute to the broadening of the EPR lines. From the exchange interaction between two dimers, a number of spin states can arise.[24] According to the spin state of the interacting dimers we can have singlet–singlet, singlet–triplet, and triplet–triplet interactions. From the last interaction, one singlet state, one triplet state, and one quintet state arise. The triplet and quintet states are split in the zero field by intra- and inter-dimer magnetic anisotropic interactions, and transitions from all of the above states should be observable through EPR spectroscopy. As a matter of fact if one is going to more carefully look at the single-crystal spectra,

(24) Snaathorst, D.; Keijzers, C. P. *Mol. Phys.* **1984**, *51*, 509.

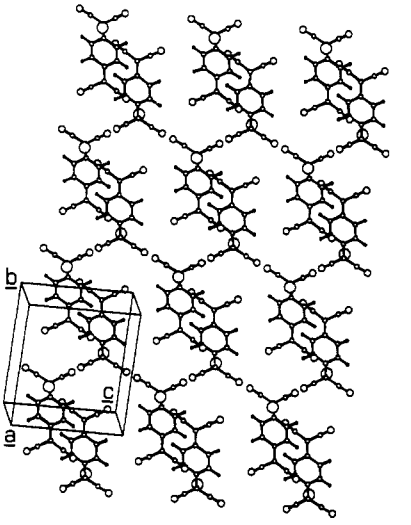

Figure 9. Schematic view of the packing of the $TCNQ^-$ ions of the B type in the *bc* plane.

some very weak additional bands overlapping the most intense ones are seen in some crystal orientations. These bands could arise from transitions between the $S = 1$ states originated by the exciton–exciton interactions, but any further analysis is experimentally impossible. A measure of the temperature dependence of the intensities of the quintet bands should allow one to estimate the separation between the spin ladders originating from the exciton–exciton interaction, but this analysis requires experiments at temperatures lower than 4.2 K that cannot be reached with sufficient accuracy.

A schematic view of the packing of the $TCNQ^-$ ions of B-type is shown in Figure 9. We see that the dinuclear units are arranged in chains: one is developing along b and the other along c. The position of the $Zn(phen)_3^{2+}$ complexes is also shown through the central zinc atoms. When the inter-dimer isotropic exchange interaction is larger than the Zeeman and anisotropic interactions, the zero field splitting tensor, $\mathbf{D}_2$, of an $S = 2$ state arising from the exchange interaction between two equivalent $S = 1$ states is given by[18]

$$\mathbf{D}_2 = (2/6)\mathbf{D}_1 + (1/3)\mathbf{D}_{11} \qquad (3)$$

where $\mathbf{D}_1$ is the zero field splitting tensor of the triplets and $\mathbf{D}_{11}$

is the zero field splitting tensor arising from the anisotropic interactions between the triplets. If these latter interactions can be approximated by a magnetic dipolar interaction, it is possible to compute $\mathbf{D}_{11}$ by using (2) and hence to obtain $\mathbf{D}_2$ to be compared with the experimental tensor. Following this approach we calculate $D_2 = 16 \times 10^{-4}$ cm^{-1} and $E_2/D_2 = 0.30$ and $D_2 = 18 \times 10^{-4}$ cm^{-1} and $E_2/D_2 = 0.15$ when the interaction between the B dimer and the next nearest neighbors along b and c, respectively, is taken into consideration. For the second choice of parameters, the computed principal axes are making $\approx 30°$ angles with the principal directions of $\mathbf{D}_1$. Although not one of the above parameters matches the experimental data, i.e., $D_1/D_2 = 1.88$ and $E_1/D_1 > E_2/D_2$, and parallel principal axes, this latter tensor seems closer to the experimental one, suggesting that an interaction can possibly occur between the B molecules along the c axis. Of course, severe approximations lie under the above model. First of all is the assumption that the exchange interaction between the dimers is larger than any other effect. If this would not be the case, the anisotropic part of the Hamiltonian will admix the quintet and singlet states arising from the triplet–triplet interaction, and the transitions observed in the crystal spectra will not be pure quintet transitions.

The EPR spectra of $Cu(phen)_3(TCNQ)_2$ show signals attributable to one unpaired electron mainly localized on one copper(II) center at any temperature. Since from the temperature dependence of the magnetic susceptibility it was evident that one of the two chains of $TCNQ^-$ ions is magnetic, which is likewise the case for $Zn(phen)_3(TCNQ)_2$ salt, some interaction between the triplet excitons and the unpaired electron localized on the copper center should occur. These interactions could be responsible for the observed temperature dependence of the g values. The principal directions of g_x and g_y at 4.2 K are affected by a large error because the g tensor becomes more axial on decreasing temperature. The z directions are the same at room temperature and at 4.2 K. Looking at the crystal structure, it is possible to see that z is parallel, within experimental error (±10°), to the CuN(12) bond, and the room temperature g_x makes an angle of 15° with Cu–N(11). The Cu–N(12) bond distance is the largest observed in the CuN_6 chromophore so that the z axes of the g tensors appear to be directed along the elongation axis of the distorted coordination octahedron.

Single-crystal EPR spectra of copper(II)-doped $Zn(phen)_3(NO_3)_2$ have been measured in 1967[25] and interpreted on a basis of a dynamic Jahn-Teller effect. The spectra showed a temperature dependence of the g tensor down to 77 K, which remained practically unchanged on lowering the temperature to 4.2 K. At 350 K, an almost isotropic spectrum was observed with $g = 2.13$. The spectrum became axial at 77 K with $g_\parallel = 2.273$ and $g_\perp = 2.064$. It is apparent that the present spectra do not follow this behavior, being *quasi*-axial at 300 K and showing a continuous g shift, particularly evident for $g_\parallel$, on decreasing the temperature at 4.2 K. The g values are $g_x = 2.05$, $g_y = 2.06$, and $g_z = 2.18$ at 4.2 K and $g_x = 2.04$, $g_y = 2.05$, and $g_z = 2.10$ at room temperature.

A possible explanation for the spectra of $Cu(phen)_3(TCNQ)_2$ is that a static Jahn–Teller distortion is operative at 300 K, modulated by cooperative effects involving the $TCNQ^-$ ions and the temperature dependence of the spectra can be ascribed to a small rearrangement of the CuN_6 chromophore, which causes a large admixture of the copper $d(x^2 - y^2)$ orbital in the ground state function to occur. Another possible explanation is to assume an interaction, very feeble on the susceptibility scale, between the electronic spin localized on copper(II) and the mobile electronic spin on the $TCNQ^-$ B-type dimer. As long as these interactions are small compared to the Zeeman term, the magnetic wavefunction of the Cu–$(TCNQ)_n$ system is properly described by a product of the copper(II) function and a radical function, and the observed g values are an average of the copper(II) g values and radical g values. The principal directions of the resulting g tensor are parallel to those of the $\mathbf{g}_{Cu}$, due to the isotropic nature of the radical $\mathbf{g}_r$ tensor. This average has to be weighted by using the relative value of the magnetic suscpetibility, i.e.

$$\mathbf{g} = (\chi_{Cu}/\chi)\mathbf{g}_{Cu} + (\chi_r/\chi)\mathbf{g}_r \quad (4)$$

where χ_{Cu} and χ_r are the expressions of the magnetic susceptibilities for an isolated copper(II) complex and a chain of radicals. Using in (4) the expressions by Hatfield et al.[26] for an alternating linear chain of $S = {}^1/_2$ spins for χ_r and a Curie law for χ_{Cu} and the best fitting values for J, the singlet-triplet splitting, and α, the alternation parameter, obtained from the fitting of the magnetic data, one obtains

$$\chi = \chi_{Cu} + \chi_r = 0.3752[g_{Cu}^2/4T + (g_r^2/T)(0.25 + 0.0214x - 0.0278x^2)/(1 + 0.853x + 0.8468x^2 - 1.749x^3)] \quad (5)$$

where $x = J/kT = 41.72/T$. In (5), we are acutally using the J and α values obtained by the fitting of the magnetic data of the zinc salt, which are those of the pure B-type dimer, since the J and α values measured from the magnetic data of the copper salt are rather inaccurate due to the large contribution of copper(II) to the overall magnetism. With these values, in fact, we compute, for example, $g_x = 2.05$, $g_y = 2.05$, and $g_z = 2.16$ at 36 K (below this temperature expression 5 loses its validity), $g_x = 2.04$, $g_y = 2.04$, and $g_z = 2.13$ at 114 K and $g_x = 2.03$, $g_y = 2.04$, $g_z = 2.11$ at 300 K, to be compared with $g_\perp = 2.04$ and $g_\parallel = 2.21$ at 36 K (powder spectra), $g_\perp = 2.04$ and $g_\parallel = 2.14$ at 114 K (powder spectra), and $g_x = 2.04$, $g_y = 2.05$, and $g_z = 2.10$ at 300 K. The agreement between the observed and the computed values is not perfect, especially for the low-temperature $g_\parallel$ value. This discrepancy can however arise from the fact that we used an average value of the magnetic susceptibility, which is actually different along the chain and perpendicular to it.

Conclusions

The single-crystal EPR spectra of $M(phen)_3(TCNQ)_2$ (M = Cu, Zn) allowed us to distinguish between the two nonequivalent dinuclear units $(TCNQ)_2^{2-}$, showing that only the unit called B is magnetic. This unit has also a peculiar B–B overlap. The spectra have also shown that at liquid-helium temperature a number of small interactions can be detected which cannot be measured with the conventional magnetic techniques. In the zinc salt the spectra showed evidence of species having S larger than 1, which can arise from magnetic exchange between localized triplet excitons, and in the copper salt some interaction between the unpaired electron of $TCNQ^-$ and the copper center was evidenced. EPR spectroscopy is still a powerful tool in investigating feeble magnetic effects, whose full characterization still demands the synthesis and the structural and magnetic characterization of other systems.

Acknowledgment. Thanks are expressed to Dr. S. Midollini and Mr. F. Cecconi for the synthesis of the compounds and the preparation of the single crystals and to Prof. D. Gatteschi for helpful discussions.

Registry No. $Zn(phen)_3(TCNQ)_2$, 119638-22-1; $Cu(phen)_3(TCNQ)_2$, 51141-11-8.

(25) Kokoszka, G. F.; Reimann, C. W.; Allen, H. C., Jr. *Inorg. Chem.* **1967**, *6*, 1657.

(26) Hall, J. W.; Weller, W. E.; Hatfield, W. E. *Inorg. Chem.* **1981**, *20*, 1033.

(27) Lowitz, D. A. *J. Chem. Phys.* **1967**, *46*, 4698.

(28) Bieber, A.; Audrê, J. *J. Chem. Phys.*, **1974**, *5*, 166.

(29) Jonkman, H. T.; van der Velde, G. A.; Nieuwpoort, W. C. *Chem. Phys. Lett.* **1974**, *25*, 62.

(30) Johansen, H. *Int. J. Quantum Chem.* **1975**, *9*, 459.